

Eccentrically loaded strip foundation on geogrid-reinforced sand

C. R. Patra^a, B. M. Das^{b,*}, M. Bhoi^c, E. C. Shin^d

^aDepartment of Civil Engineering, National Institute of Technology, Rourkela 769008, India

^bCollege of Engineering and Computer Science, California State University,
Sacramento, CA, 95819, USA

^cDepartment of Civil Engineering, National Institute of Technology, Rourkela 769008, India

^dDepartment of Civil Engineering, University of Incheon, Incheon Metropolitan City, Korea, 402-749

ABSTRACT: Results are presented for laboratory model tests conducted to determine the ultimate bearing capacity of an eccentrically loaded strip foundation supported by geogrid-reinforced sand. Only one type of sand at one relative density of compaction and one type of geogrid were used for the tests. The depth of the foundation was varied from zero to B (width of foundation). Based on the laboratory test results, an empirical relationship called reduction factor has been suggested that correlates the ratio of the ultimate bearing capacity of an eccentrically loaded foundation with that for a foundation where the load is applied centrally.

Keywords: Eccentric loading; geogrid; sand; strip foundation; ultimate bearing capacity

1. Introduction

During the last two decades, the results of a number of studies have been published relating to the ultimate bearing capacity of shallow foundations supported by multi-layered geogrid-reinforced sand. The results were mostly obtained from small-scale laboratory model tests (Omar

*Corresponding author. Tel: +1 916 278 6127; fax: +1 916 278 5949.

E-mail address: dasb@csus.edu (B.M. Das)

et al., 1993; Yetimoglu et al., 1994; Das and Omar, 1994; Khing et al., 1992; Adam and Collin, 1997). Most of the experimental studies cited above were conducted for surface foundation condition (that is, depth of foundation, $D_f = 0$). Shin and Das (2000) provided the results of a limited number of laboratory model studies for the ultimate bearing capacity of strip foundations with D_f/B (B = width of foundation) greater than zero. None of the published studies, however, address the effect of load eccentricity on the ultimate bearing capacity. The purpose of this paper is to report some recent laboratory bearing capacity test results on eccentrically loaded strip foundations with D_f/B varying from zero to one.

2. Eccentrically loaded strip foundation on unreinforced sand

Meyerhof (1953) proposed a semi-empirical procedure to estimate the ultimate bearing capacity of a shallow foundation subjected to eccentric load that is generally referred to as the equivalent area method. According to this method, the average ultimate bearing capacity, $q_{u(e)}$, of a strip foundation on unreinforced sand is given as,

$$q_{u(e)} = \frac{Q_u}{B} = \left[qN_q F_{qd} + \frac{1}{2} \gamma B' N_\gamma F_{\gamma d} \right] \frac{B'}{B} \quad (1)$$

where $q_{u(e)}$ = ultimate bearing capacity with load eccentricity e ; Q_u = ultimate load per unit length of foundation; $q = \gamma D_f$; γ = unit weight of soil; D_f = depth of foundation; B = width of foundation; $B' = B - 2e$; e = load eccentricity; N_q, N_γ = bearing capacity factors; $F_{qd} = F_{\gamma d}$ = depth factors (Meyerhof, 1963) = $1 + 0.1 (D_f/B) \tan(45 + \phi'/2)$; ϕ' = friction angle of sand.

Prakash and Saran (1971) provided a comprehensive mathematical formulation to estimate the ultimate bearing capacity of a rough strip foundation under eccentric loading. According to this theory, for a strip foundation on sand,

$$q_{u(e)} = qN_{q(e)} + \frac{1}{2}\gamma BN_{\gamma(e)} \quad (2)$$

where $N_{q(e)}$ and $N_{\gamma(e)}$ = bearing capacity factors = $f(\varphi', e/B)$.

The above equation does not include the depth factors as shown in Eq 1.

Purkayastha and Char (1977) carried out the stability analysis of an eccentrically loaded strip foundation on sand using the method of slices proposed by Janbu (1957). Based on this study, they proposed that,

$$\frac{q_{u(e)}}{q_{u(e=0)}} = 1 - R_K \quad (3)$$

where R_K = the reduction factor = $\alpha\left(\frac{e}{B}\right)^K$ (4)

Based on a statistical analysis, it was also shown that B and φ' have no influence on R_K . The variations of α and K determined by this study are summarized in Table 1. The magnitude of α decreases with the increase in D_f/B up to a minimum of $D_f/B = 0.5$ and increases thereafter. From this table it can be seen that the average values of α and K are, respectively, 1.81 and 0.8. For $D_f/B = 0$ and $e/B < 0.2$, this solution provides practically the same results as the equivalent area method suggested by Meyerhof (1953).

3. Foundation on geogrid-reinforced sand

A reliable procedure for estimating the ultimate bearing capacity under centric loading for a strip foundation supported by geogrid-reinforced sand is yet to be developed. Takemura et al. (1992) conducted several centrifuge tests for surface foundation to determine the ultimate bearing capacity of a strip foundation on geogrid-reinforced sand. Based on the model tests they concluded that, just before the load intensity reached its peak, a rigid soil block is formed under

the foundation and this block behaves as if it were an embedded foundation. Based on this observation, the failure mode is shown in Fig.1. In this figure Q_{uR} is the ultimate load per unit length of the foundation. Thus, the ultimate bearing capacity without depth factor can conservatively be given as,

$$q_{uR} = d\gamma N_\gamma + \frac{1}{2}\gamma BN_\gamma \quad (5)$$

where q_{uR} = ultimate bearing capacity on geogrid-reinforced sand; B = width of geogrid layer; d = depth of reinforcement below the bottom of the foundation.

The reinforcement depth below the bottom of the foundation can be expressed as,

$$d = u + (N - 1)h \quad (6)$$

where u = depth of first layer of geogrid from the bottom of the foundation h = distance between consecutive layers of reinforcement; N = number of geogrid layers.

Assuming the failure mechanism under centric load as shown in Fig.1 to be correct, it appears that the ultimate bearing capacity due to eccentric loading (Figure 2) may be expressed in a form similar to Eq 3. Or,

$$\frac{q_{uR(e)}}{q_{uR}} = 1 - R_{KR} \quad (7)$$

where $q_{uR(e)}$ = ultimate bearing capacity due to eccentric loading, R_{KR} = reduction factor for geogrid-reinforced sand.

In Fig. 2, $Q_{uR(e)}$ is the ultimate load per unit length of the foundation with a load eccentricity e , and D_f is the depth of the foundation. The reduction factor may be expressed as

$$R_{KR} = \alpha_1 \left(\frac{d_f}{B} \right)^{\alpha_2} \left(\frac{e}{B} \right)^{\alpha_3} \quad (8)$$

where α_1 , α_2 , and α_3 are constants and $d_f = D_f + d$.

4. Laboratory model tests

The model foundation used for this study had a width of 80 mm and a length of 360 mm. It was made out of a mild steel plate with a thickness of 25 mm. The bottom of the model foundation was made rough by coating it with glue and then rolling it over sand. Bearing capacity tests were conducted in a box measuring 0.8m (length) \times 0.365m (width) \times 0.7m (depth). The inside walls of the box and the edges of the model were polished to reduce friction as much as possible. The sides of the box were heavily braced to avoid lateral yielding. Locally available sand dried in an oven was used for the present model tests. The sand used for the tests had 100% passing 0.7-mm size sieve and 0% passing 0.3-mm size sieve. It had an effective size (D_{10}) of 0.41 mm and a uniformity coefficient (C_u) of 1.4. For all tests, the average unit weight and the relative density of compaction were kept at 14.81 kN/m³ and 72%, respectively. The average peak friction angle ϕ' of the sand at the test conditions as determined from direct shear tests was 42.4°. Tensar biaxial geogrid (BX1100) was used for the present tests. The physical properties of the geogrid are given in Table 2.

In conducting a model test, sand was placed in lifts of 25 mm in the test box. For each lift, the amount of soil required to produce the desired unit weight was weighed and compacted using a flat bottomed wooden block. Geogrid layers were placed in the sand at desired values of u/B and h/B . The model foundation was placed on the surface as well as at desired depths below the surface of the sand bed. Centric or eccentric load to the model foundation was applied through an electrically operated hydraulic jack. Two dial gauges having 0.01-mm accuracy placed on either side of the model foundation recorded the settlement of the foundation. Load was applied in small increments and the resulting deformations recorded so that the entire load-settlement curve could be obtained. Since the length of the model foundation was approximately the same as the

width of the test box, it can be assumed that an approximate plane strain condition did exist during the tests.

For the present test program, the following parameters were adopted for the geogrid reinforcement layers: $u/B = 0.35$, $h/B = 0.25$, $b/B = 5$. The sequence of the model tests is given in Table 3.

5. Model test results

For any given test, at any time during the test, the load per unit area on the model foundation [q_R or $q_{R(e)}$] can be given as Q/A (Q = load on the foundation, A = area of foundation). Figure 3 shows typical plots of load per unit area $q_{R(e)}$ versus foundation settlement (tests 31 through 33) obtained from the model test program. The plots were typical local shear types of failure such as those described by Vesic (1973). The ultimate bearing capacities determined from the load-displacement plots are shown in Fig.4. It needs to be pointed out that the values of tensile strength and stiffness were not scaled down to be consistent with geometric scaling. As expected, for any given D_f/B (or d_f/B), the magnitudes of $q_{uR(e)}$ decreased with the increase in e/B . Also, for any given D_f/B and e/B , the ultimate bearing capacity increased with the increase in d_f/B .

According to Eq 8, the reduction factor,

$$R_{KR} \propto \left(\frac{e}{B} \right)^{\alpha_3} \quad (9)$$

Using the experimental ultimate bearing capacities $q_{uR(e)}$ shown in Fig.4, the reduction factors were calculated and these are shown in Figs.5a, 5b, and 5c. From these figures it can be seen that, for any given D_f/B and d_f/B , the plot of R_{KR} versus e/B is approximately a straight line in a log-log plot. The average value of α_3 is about 1.21. Thus,

$$R_{KR} \propto \left(\frac{e}{B}\right)^{1.21} \quad (10)$$

Again, Fig. 6 shows the plots of R_{KR} versus d_f/B for $e/B = 0.05, 0.10,$ and 0.15 . Although there is some scatter as expected, the slope of the average lines for all e/B values (that is, α_2 is approximately equal to -0.12 . Thus,

$$R_{KR} = \alpha_1 \left(\frac{d_f}{B}\right)^{-0.12} \left(\frac{e}{B}\right)^{1.21} \quad (11)$$

or,

$$\alpha_1 = \frac{R_{KR}}{\left(\frac{d_f}{B}\right)^{-0.12} \left(\frac{e}{B}\right)^{1.21}} \quad (12)$$

Using the average lines for each e/B shown in Fig. 6, the magnitudes of α_1 were calculated. These deduced values of α_1 are plotted against the corresponding e/B in Fig. 7. The average value of α_1 from this plot is about 4.97. Thus,

$$R_{KR} \approx 4.97 \left(\frac{d_f}{B}\right)^{-0.12} \left(\frac{e}{B}\right)^{1.21} \quad (13)$$

It needs to be pointed out that the present tests were conducted with one model footing and one type of sand. The existence of possible scale effects by changing the width of the foundation has not been verified. This may lead to changes in the magnitudes of the constants $\alpha_1, \alpha_2,$ and α_3 .

6. Conclusions

A limited number of laboratory model test results for the ultimate bearing capacity of eccentrically loaded strip foundations supported by sand reinforced with multi-layers of geogrid has been presented. The eccentricity ratio (e/B) was varied from zero to 0.15 along with the

foundation embedment ratio (D_f/B) from zero to one. Based on the model test results, the following conclusions can be drawn:

1. For similar reinforcement conditions, the ratio of the ultimate bearing capacity of eccentrically loaded foundations to that for loaded centrally can be related by a reduction factor.
2. The reduction factor is a function of d_f/B and e/B .

References

- Adams, M. T. and Collin, J. C., 1977. Large model spread footing load tests on geogrid-reinforced soil foundations. *Journal of Geotechnical and Geoenvironmental Engineering ASCE*, 123, (1), 66-72.
- Das, B. M. and Omar, M. T., 1994. The effects of foundation width on model tests for the bearing capacity of sand with geogrid reinforcement. *Geotechnical and Geological Engineering* 12(2), 133-141.
- Janbu, N., 1957. Earth pressure and bearing capacity calculations by generalized procedure of slices. *Proceedings of the Fourth International Conference on Soil Mechanics and Foundation Engineering*, London 2, 207-212.
- Khing, K. H., Das, B. M., Puri, V. K., Cook, E. E., and Yen, S. C., 1993. The bearing capacity of a strip foundation on geogrid-reinforced sand. *Geotextiles and Geomembranes* 12(4), 351-361.
- Meyerhof, G. G., 1953. The bearing capacity of footing under eccentric and inclined loads. *Proceedings of the Third International Conference on Soil Mechanics and Foundation Engineering*, Zurich 1, 440-444.

- Meyerhof, G. G., 1963. Some recent research on the bearing capacity of foundations. *Canadian Geotechnical Journal* 1(1), 16-26.
- Omar, M. T., Das, B. M., Puri, V. K. and Yen, S. C., 1993. Ultimate bearing capacity of shallow foundations on sand with geogrid reinforcement. *Canadian Geotechnical Journal* 30(3), 545-549.
- Prakash, S. and Saran S., 1971. Bearing capacity of eccentrically loaded footing. *Journal of the Soil Mechanics and Foundations Division, ASCE* 97(1), 95-117.
- Purkayastha, R. D. and Char, R. A. N., 1977. Stability analysis for eccentrically loaded footings. *Journal of the Geotechnical Engineering Division, ASCE* 103(6), 647-651.
- Shin, E. C. and Das, B. M., 2000. Experimental study of bearing capacity of a strip foundation on geogrid-reinforced sand. *Geosynthetics International* 7(1), 59-71.
- Takemura, J., Okamura, M., Susmasa, N., and Kimura, T., 1992. Bearing capacities and performance of sand reinforced with geogrids. *Proceedings of the International Symposium on Earth Pressure Practice, Fukuoka, Balkema* 1, 695-700.
- Vesic, A.S., 1973. Analysis of ultimate loads on shallow foundations. *Journal of the Soil Mechanics and Foundations Division, ASCE* 99(1) 45-73.
- Yetimoglu, T., Wu, J. T. H. and Saglamer, A., 1994. Bearing capacity of rectangular footings on geogrid-reinforced sand. *Journal of the Geotechnical Engineering Division, ASCE* 120(12) 2083-2089.

LIST OF SYMBOLS

B = foundation width

$B' = B = 2e$ = effective foundation width

D_f = depth of foundation

d = depth of reinforcement measured from the bottom of the foundation

$d_f = d + D_f$

e = eccentricity

$F_{qd}, F_{\gamma d}$ = depth factors

H = distance between two consecutive geogrid layers

K = a constant

N = number of geogrid layers

$N_q, N_{q(e)}, N_\gamma, N_{\gamma(e)}$ = bearing capacity factors

$q = \gamma D_f$

$q_{u(e)}, q_{u(e=0)}$ = ultimate bearing capacity on unreinforced sand, respectively, with load eccentricity, e , and $e = 0$

$q_{uR(e)}, q_{uR}$ = ultimate bearing capacity on reinforced sand, respectively, with load eccentricity, e , and $e = 0$

Q = load per unit area

Q_u = ultimate load per unit length (unreinforced sand)

R_K, R_{KR} = reduction factor for unreinforced and reinforced case, respectively

U = distance between the bottom of the foundation and the first geogrid layer

$\alpha, \alpha_1, \alpha_2, \alpha_3$ = constants

γ = unit weight of sand

ϕ' = drained friction angle of sand

Table 1. Variations of α and K (Eq 4).

$\frac{D_f}{B}$	α	K
0	1.862	0.73
0.25	1.811	0.785
0.5	1.754	0.80
1.0	1.820	0.888

Table 2. Physical properties of the geogrid.

Parameters	Quantity
Structure	Punctured sheet drawn
Polymer	PP/DHPE copolymer
Junction method	Unitized
Aperture size (MD/XMD)	25.4 mm/33.02 mm
Rib thickness	0.762 mm
Junction thickness	2.79 mm
Tensile modulus @ 2% elongation (MD)	204.3 kN/m
Tensile modulus @ 2% elongation (XMD)	291.9 kN/m
Junction strength (MD)	11.2 kN/m
Junction strength (XMD)	18.4 kN/m

Table 3. Sequence of model tests.

Test No.	D_f/B	N	d_f/B	e/B
1-3	0	2, 3, 4	0.6, 0.85, 1.1	0
4-6	0	2, 3, 4	0.6, 0.85, 1.1	0.05
7-9	0	2, 3, 4	0.6, 0.85, 1.1	0.10
10-12	0	2, 3, 4	0.6, 0.85, 1.1	0.15
13-15	0.5	2, 3, 4	1.1, 1.35, 1.6	0
16-18	0.5	2, 3, 4	1.1, 1.35, 1.6	0.05
19-21	0.5	2, 3, 4	1.1, 1.35, 1.6	0.10
22-24	0.5	2, 3, 4	1.1, 1.35, 1.6	0.15
25-27	1.0	2, 3, 4	1.6, 1.85, 2.1	0
28-30	1.0	2, 3, 4	1.6, 1.85, 2.1	0.05
31-33	1.0	2, 3, 4	1.6, 1.85, 2.1	0.10
34-36	1.0	2, 3, 4	1.6, 1.85, 2.1	0.15

Note: $u/B = 0.35$, $h/B = 0.25$, and $b/B = 5$ for all tests on reinforced sand.

LIST OF FIGURES

- Fig. 1 Assumed failure mode under a centrally loaded surface strip foundation on geogrid-reinforced sand
- Fig. 2 Assumed failure mode under an eccentrically loaded strip foundation on geogrid-reinforced sand
- Fig. 3 Plot of load per unit area versus settlement— $D_f/B = 1$ (tests 31, 32, 33)
- Fig. 4 Variation of $q_{UR(e)}$ with e/B and d_f/B —(a) $D_f/B = 0$ (tests 1 through 12); (b) $D_f/B = 0.5$ (tests 13 through 24); (c) $D_f/B = 1.0$ (tests 25 through 36)
- Fig. 5 Plot of R_{KR} versus e/B
- Fig. 6 Plot of R_{KR} versus d_f/B for $e/B = 0.05, 0.10, \text{ and } 0.15$
- Fig. 7 Plot of α_1 versus e/B

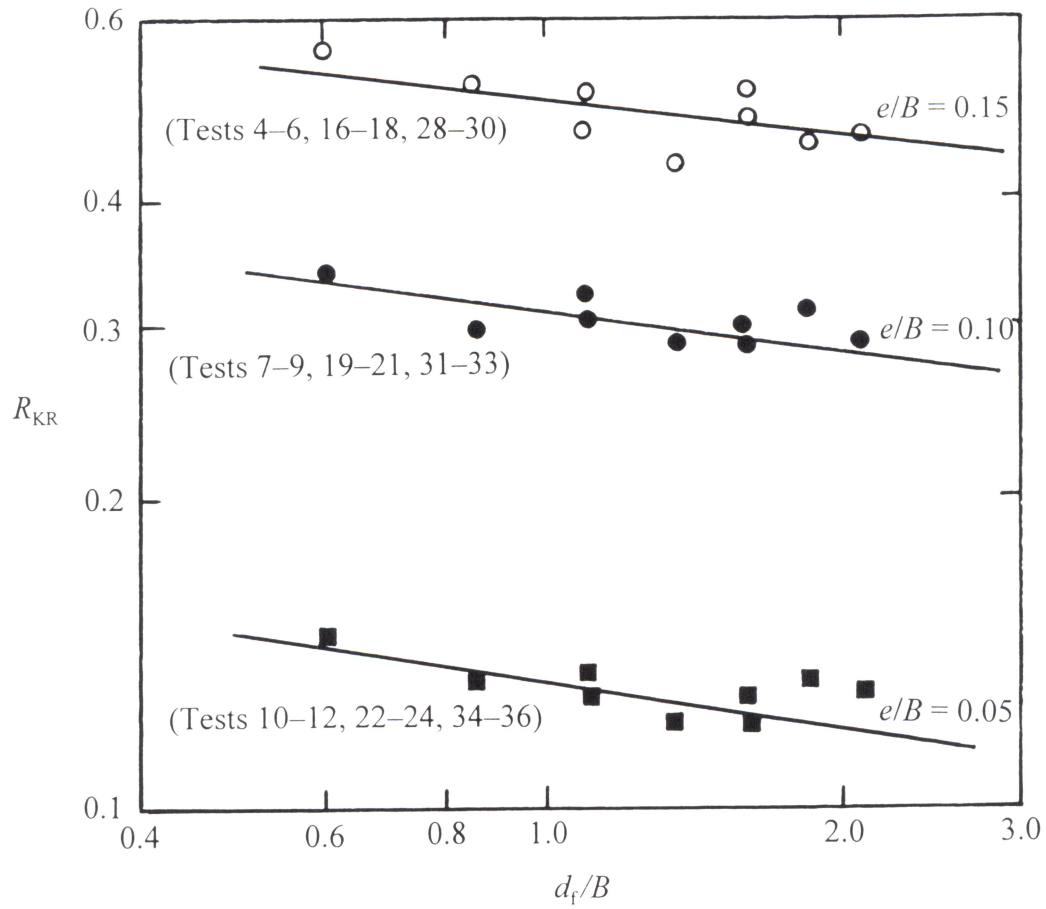


Fig. 6 Plot of R_{KR} versus d_f/B for $e/B = 0.05, 0.10, \text{ and } 0.15$

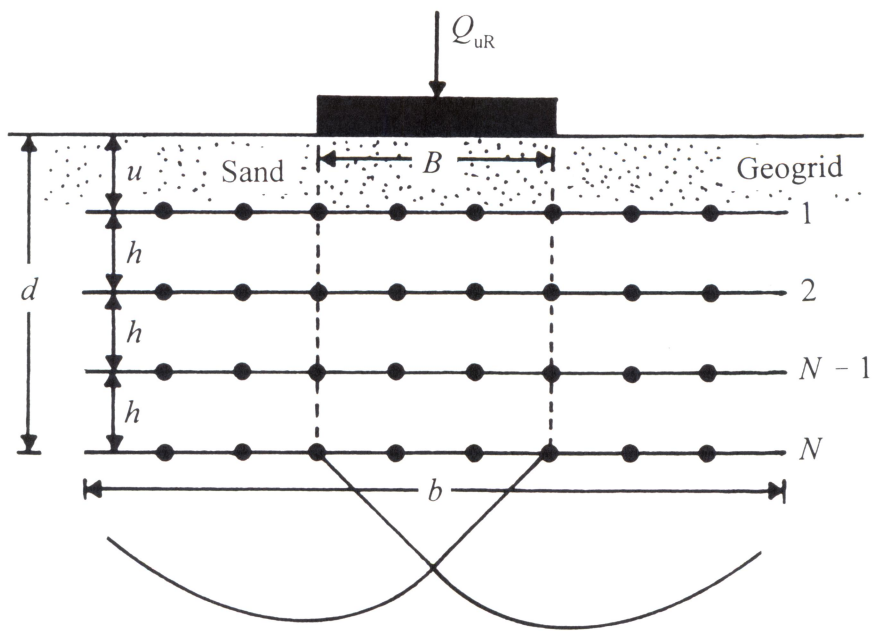


Fig. 1 Assumed failure mode under a centrally loaded surface strip foundation on geogrid-reinforced sand

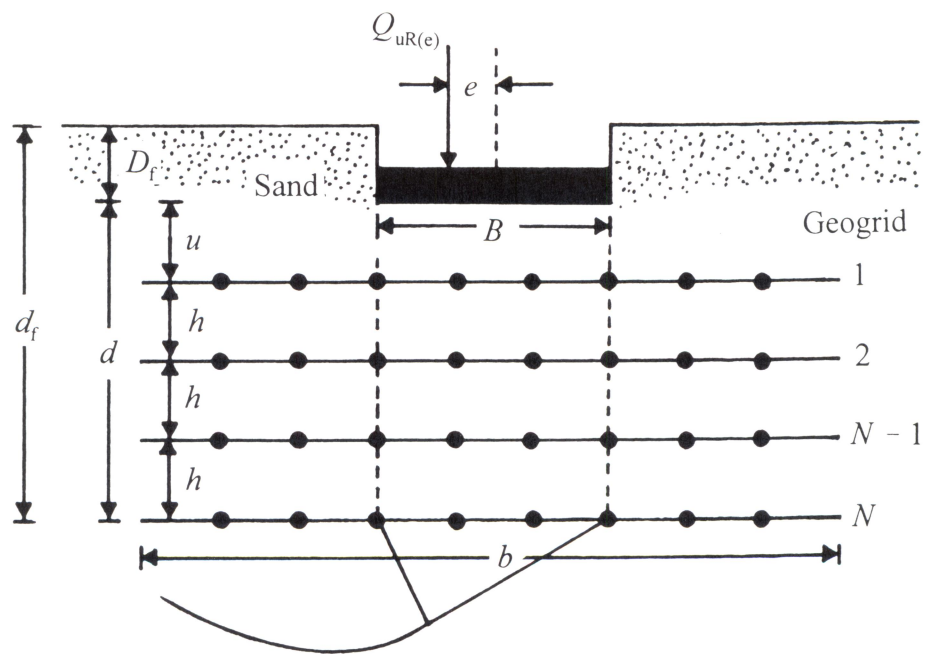


Fig. 2 Assumed failure mode under an eccentrically loaded strip foundation on geogrid-reinforced sand

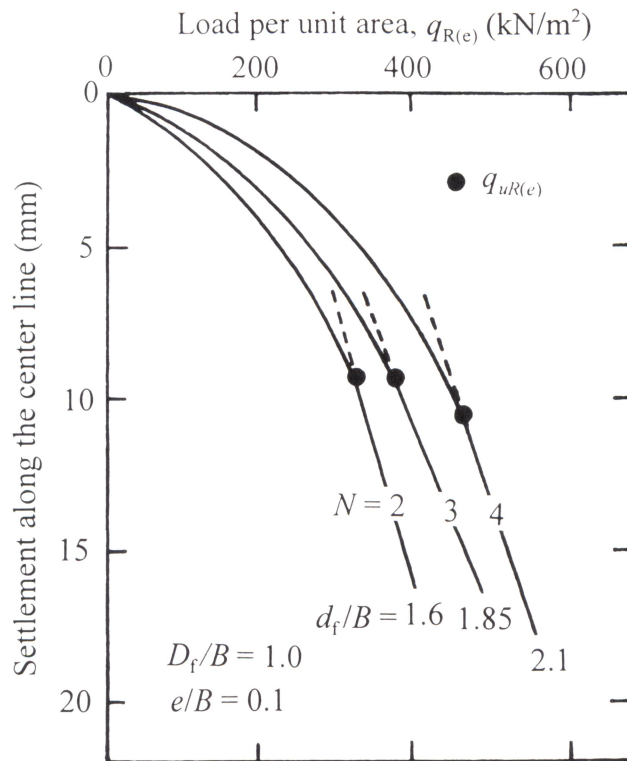


Fig. 3 Plot of load per unit area versus settlement— $D_f/B = 1$ (tests 31, 32, 33)

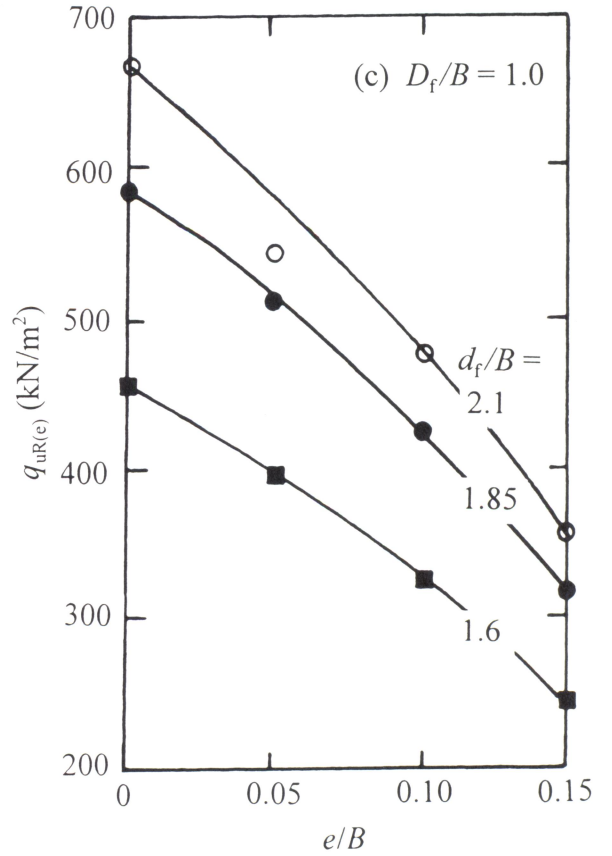
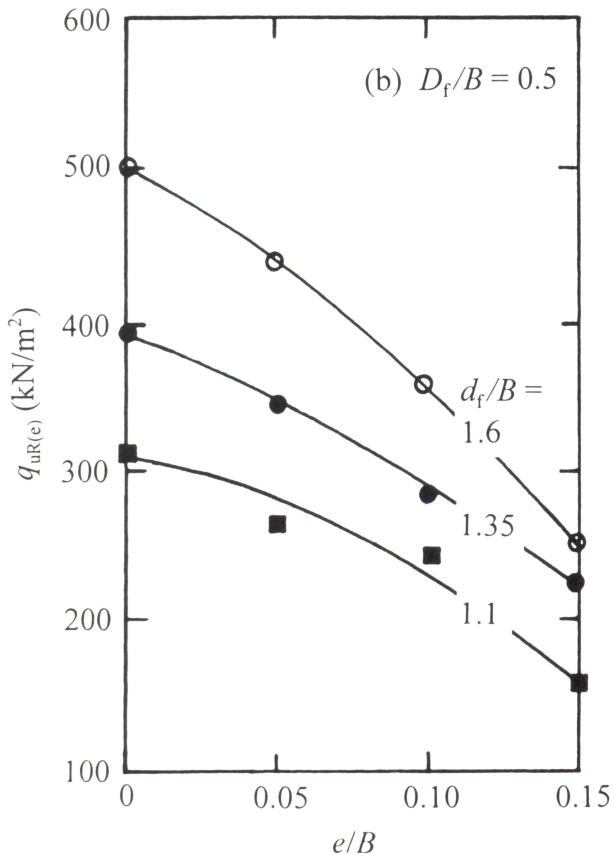
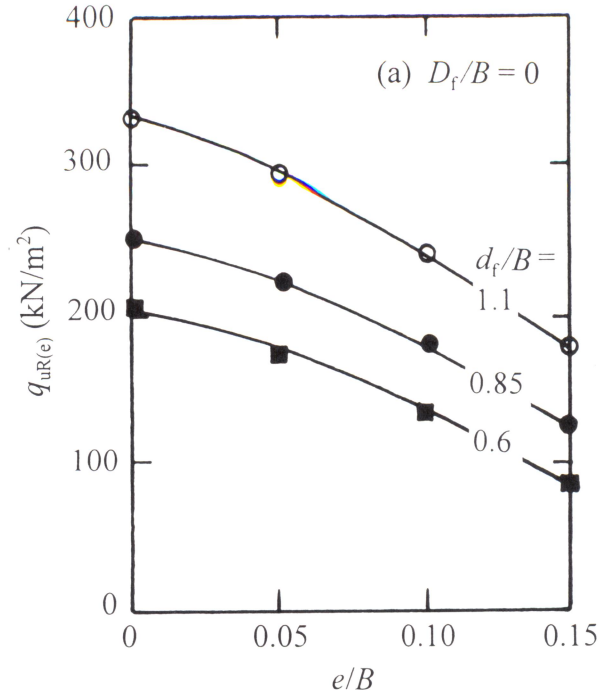


Fig. 4 Variation of $q_{UR(e)}$ with e/B and d_f/B —(a) $D_f/B = 0$ (tests 1 through 12);
 (b) $D_f/B = 0.5$ (tests 13 through 24); (c) $D_f/B = 1.0$ (tests 25 through 36)

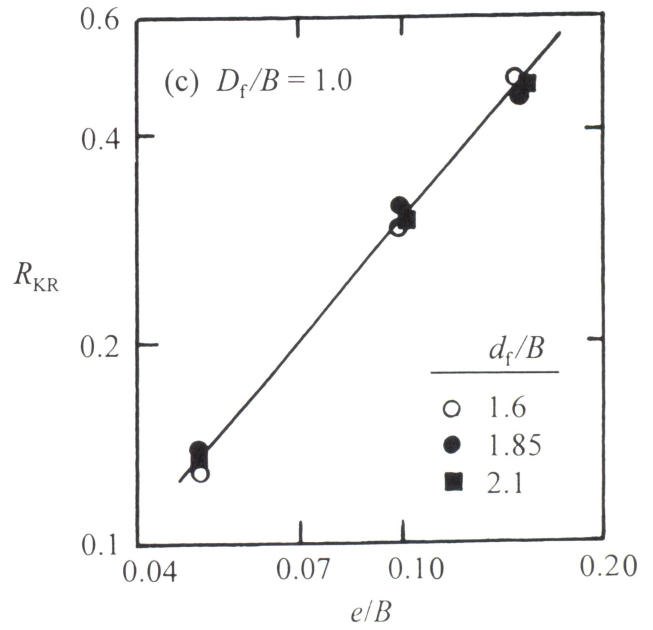
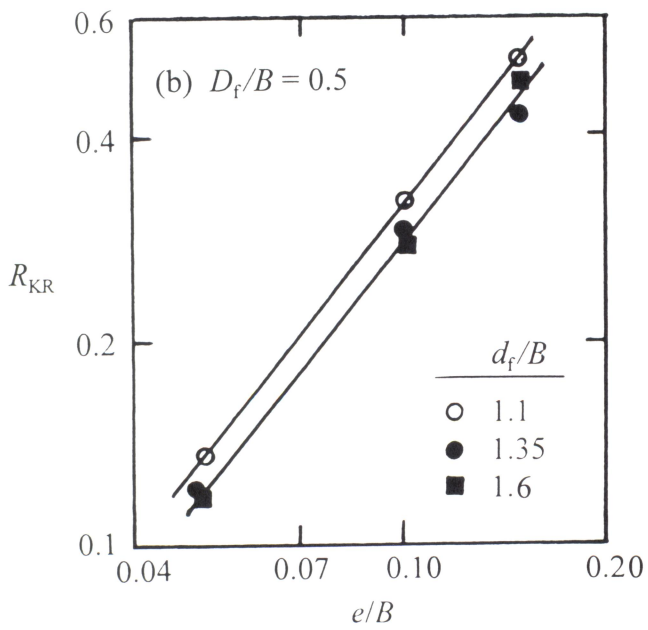
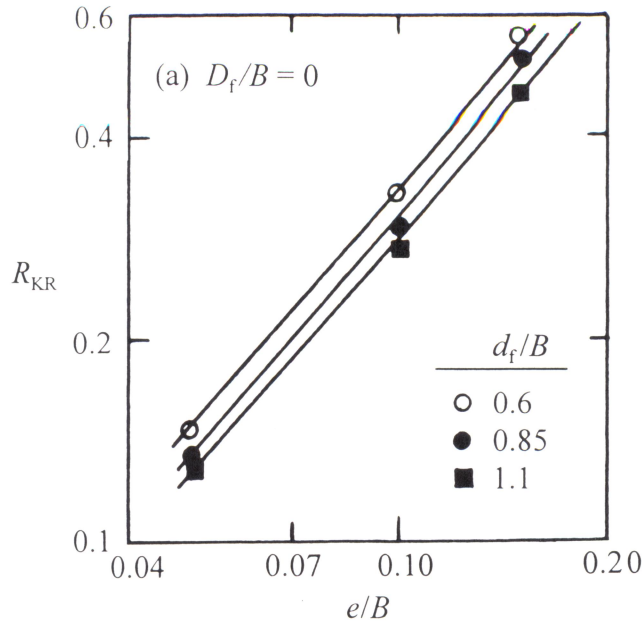


Fig. 5 Plot of R_{KR} versus e/B

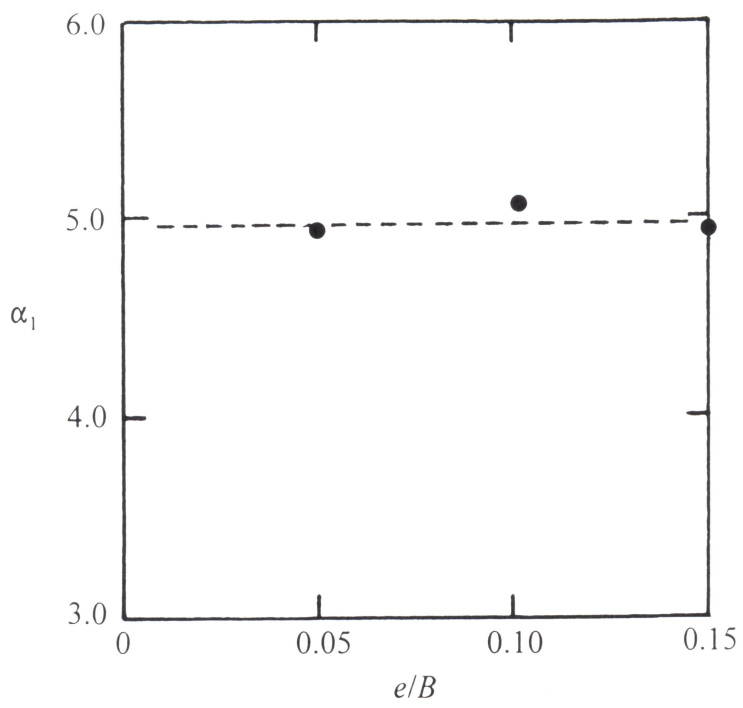


Fig. 7 Plot of α_1 versus e/B